Iterative trace reconstruction of aliased radio-frequency data obtained using harmonic imaging

A feasibility study

Van Neer, P. L.M.J.; Vos, H. J.; Volker, A. F.W.

DOI
10.1109/ULTSYM.2017.8091691

Publication date
2017

Document Version
Accepted author manuscript

Published in
2017 IEEE International Ultrasonics Symposium, IUS 2017

Iterative trace reconstruction of aliased radio-frequency data obtained using harmonic imaging: a feasibility study

P.L.M.J. van Neer[1], H.J. Vos[2,3], A.F.W. Volker[1]
[1]*Department of Acoustics and Sonar, TNO, the Hague, the Netherlands*
[2]*Acoustical Wavefield Imaging, ImPhys, Delft University of Technology, the Netherlands*
[3]*Biomedical Engineering, Erasmus MC, Rotterdam, the Netherlands;*
paul.vanneer@tno.nl

***Abstract*— It is critical to use a proper spatial sampling, otherwise images suffer from grating lobes. However, the cost of a medical ultrasound scanner is strongly related to the channel count of the receive electronics. This has led to channel reduction using multiplexing or in-probe pre-beamforming methods at the cost of image quality or frame rate. An alternative is to reduce the receive channel count and reconstruct the non-aliased data from spatially aliased data. Last year we reported on a wavenumber frequency domain mapping based iterative trace reconstruction method developed for fundamental imaging. However, harmonic imaging is often used in medical imaging to further improve the image quality. As the reconstruction method assumes linearity, it is not a-priori clear whether the reconstruction will work satisfactory in combination with harmonic imaging. Here, the feasibility of using the method for harmonic imaging is investigated using *in-vivo* linear array data. The reconstruction algorithm operates by iteratively focusing and defocusing of the data using an imaging algorithm and uses intermittent thresholding to suppress the aliasing artifacts in the imaging domain. Properly sampled plane wave transmission datasets were recorded of the right common carotid artery of a healthy volunteer using a linear array transducer attached to a research system. The reconstruction technique significantly improved the image quality of all aliased datasets for both the fundamental and second harmonic imaging modalities. In fact, the reconstruction quality was slightly better for the second harmonic imaging case.**

Keywords—imaging; aliasing; wavenumber-frequency domain mapping; Stolt migration; channel reduction

I. INTRODUCTION

It is critical to use a proper spatial sampling, otherwise images suffer from grating lobes. However, the cost of a medical ultrasound scanner is strongly related to the channel count of the receive electronics. This has led to channel reduction using multiplexing or in-probe pre-beamforming methods at the cost of image quality or frame rate [1]. An alternative is to reduce the receive channel count and reconstruct the non-aliased data from spatially aliased data. Last year we reported on a wavenumber frequency domain mapping (Stolt migration) based iterative trace reconstruction method developed for fundamental imaging. However, the de-facto standard in medical imaging is second harmonic imaging. Since the reconstruction algorithm assumes linearity it is not a-priori clear whether the algorithm will function satisfactory in combination with the second harmonic imaging modality. Here, the feasibility of using the method for harmonic imaging is investigated using *in-vivo* linear array data obtained of the right common carotid artery of a healthy volunteer.

II. THE RECONSTRUCTION METHOD

The algorithm to reconstruct spatially undersampled data to data with a sufficient spatial sampling [2,3] consisted of the following iterative operations:

1. Empty traces were placed at locations requiring interpolated signals.
2. An imaging algorithm was applied to focus the waves in the entire dataset.
3. The Hilbert transform was used to compute the envelope of the radio-frequency signals
4. The aliasing noise in the signals was suppressed by use of an amplitude threshold.
5. The imaging algorithm was inversely applied to defocus the waves in the entire dataset.
6. The empty traces were replaced with the reconstructed traces.

Steps 2 – 6 were repeated iteratively using a successively lower threshold in step 4. When the threshold became lower than the noise level in the data, the scheme halted. The imaging algorithm applied in this work was a wavenumber-frequency domain mapping also known as Stolt migration [4,5].

In the aforementioned algorithm the following assumptions were made:

- the data represented acoustic waves,
- the wavefield could be focused,
- the data was equidistantly sampled in time and space,

- the effect of diffraction during the receive path was significantly higher compared to the effect of diffraction during the transmission path,
- the backscatter amplitude was sufficiently low such that the backpropagation could be considered to be linear.

For a more extensive description of the reconstruction algorithm the reader is referred to [2,3].

III. Experimental setup

Ultrasonic radio-frequency signals were recorded of the right common carotid artery of a healthy volunteer using a linear phased array transducer (L7-4 probe, 5 MHz center frequency, 128 elements, pitch 0.3 mm) connected to a Verasonics Vantage 256 research scanner (Kirkland, WA, USA). Plane wave transmissions were used. The frequency used for fundamental imaging was 5 MHz, whereas the fundamental frequency used for second harmonic imaging was 3.4 MHz. In the case of second harmonic imaging pulse-inversion was applied. The imaging algorithm consisted of a wavenumber-frequency domain mapping also known as Stolt migration [4,5]. Aliased datasets were created by undersampling the spatial-aliasing-free datasets by a factor of 2, 4 and 8. These aliased datasets were subsequently used to evaluate the reconstruction algorithm.

IV. Results and Discussion

A. *Fundamental imaging*

Imaged datasets obtained using fundamental imaging are shown in Fig. 1. The imaged original dataset is shown in Fig. 1a, the imaged aliased datasets are shown in Figs. 1b, 1d and 1f, and the imaged reconstructed datasets are shown in Figs. 1c, 1e and 1g. The averaged intensities of the green squares in each figure is provided in Table I.

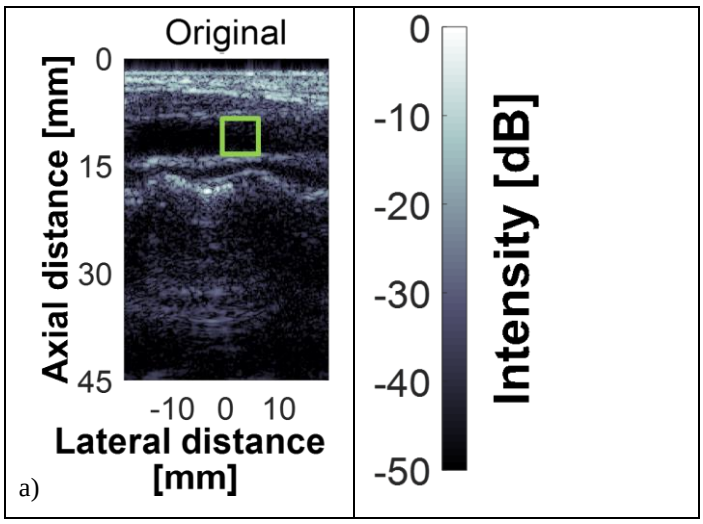

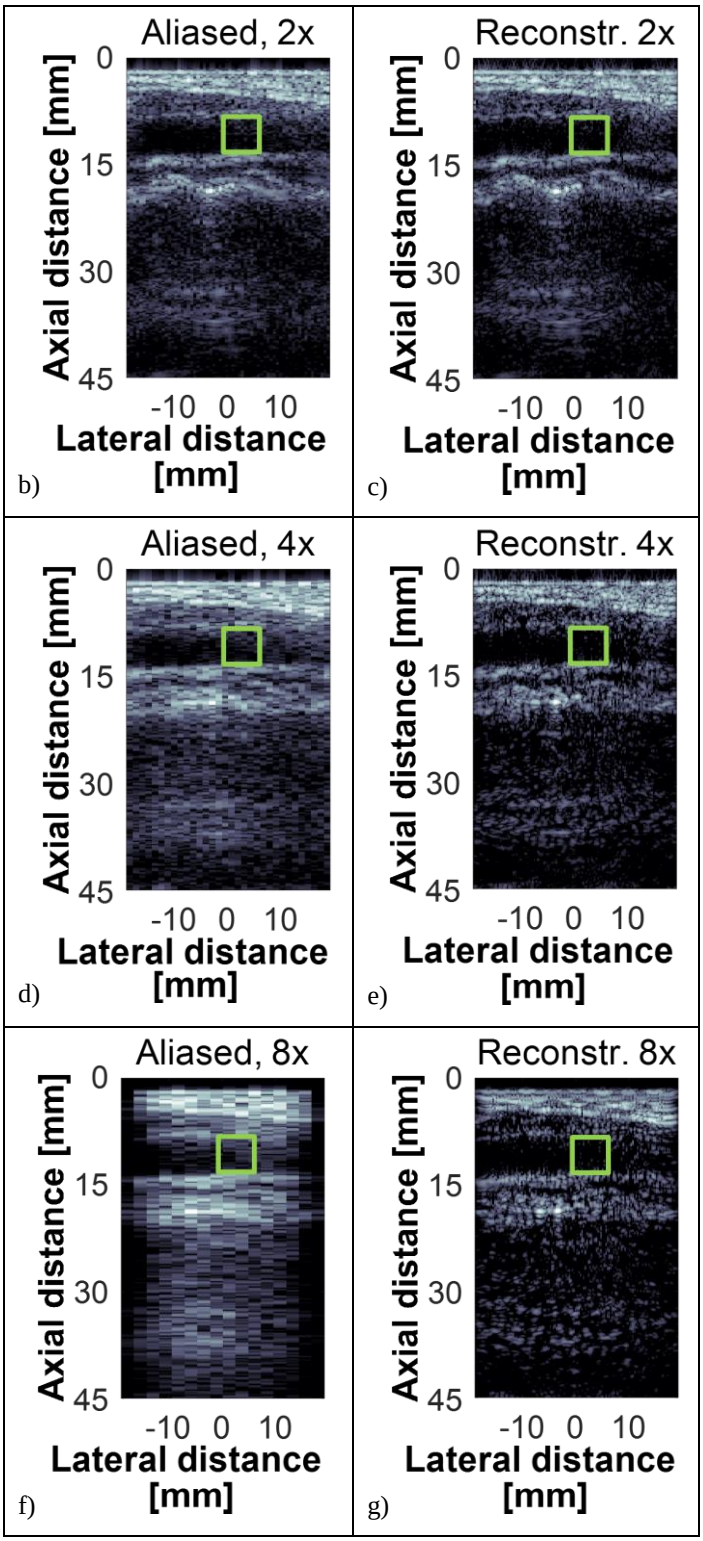

Fig. 1. Imaged original, aliased and reconstructed datasets obtained using fundamental imaging. The green rectangle denotes the area where the intensty is analyzed in Table I. a) Original dataset. b) Dataset with 2x channel reduction. c) Reconstruction based on dataset with 2x channel reduction. d) Dataset with 4x channel reduction. e) Reconstruction based on dataset with 4x channel reduction. f) Dataset with 8x channel reduction. g) Reconstruction based on dataset with 8x channel reduction.

As can be observed in Fig. 1, the imaged aliased datasets became increasingly washed out and blocky for higher levels of channel reduction. At each level of channel reduction the imaged reconstructed datasets were significantly clearer and sharper compared to the imaged aliased datasets. For higher levels of channel reduction the details in the imaged reconstructed datasets became less distinct and the images more grainy. This was caused by the increasing effect as a function of channel reduction level of the numerical noise introduced into the images due to the iterative forward and inverse applications of the imaging algorithm. Notice the hyperbola-like artifacts in the near-field of the reconstructed image based on the 8x aliased dataset.

Table I shows the average intensity of the green squares in the corresponding figures of Fig. 1.

TABLE I. AVERAGE INTENISTY IN GREEN SQUARES IN FIG. 1

Channel reduction level	**Aliased image [dB]**	**Reconstructed image [dB]**
2x	-44 (Fig. 1b)	-44 (Fig. 1c)
4x	-41 (Fig. 1d)	-44 (Fig. 1e)
8x	-41 (Fig. 1f)	-45 (Fig. 1g)
Original	-47 (Fig. 1a)	

The averaged intensities in the green squares in the imaged reconstructed datasets were equal to or lower than the corresponding intensities in the imaged aliased datasets. However, the reconstructed intensities remained higher than the one of the original dataset, which was caused by the increased blurring of the edges of the blood vessel in the imaged reconstructed dataset.

B. Second harmonic imaging

Imaged datasets obtained using 2nd harmonic imaging and pulse-inversion are shown in Fig. 2. The imaged original dataset is shown in Fig. 2a, the imaged aliased datasets are shown in Figs. 2b, 2d and 2f, and the imaged reconstructed datasets are shown in Figs. 2c, 2e, and 2g. The average intensities of the green squares in each figure is provided in Table II.

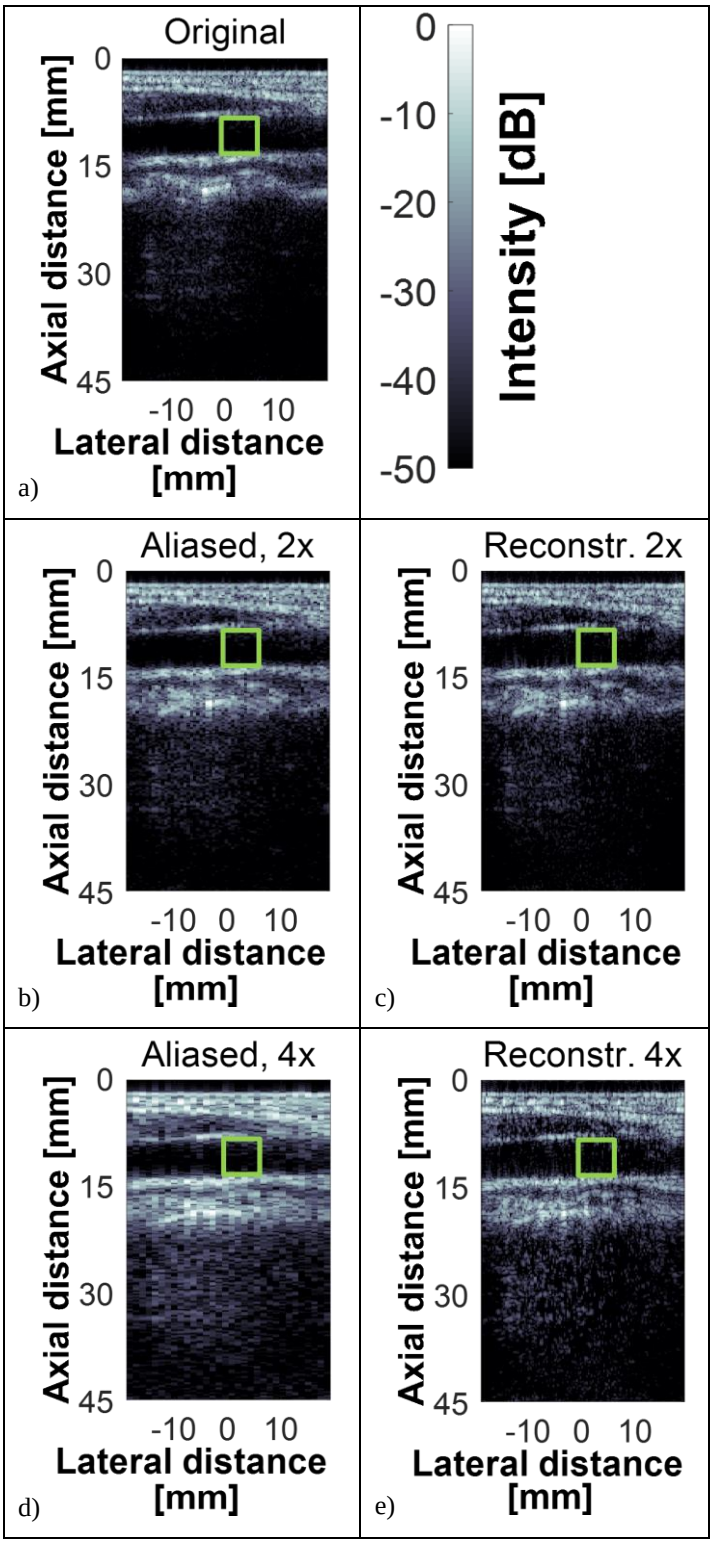

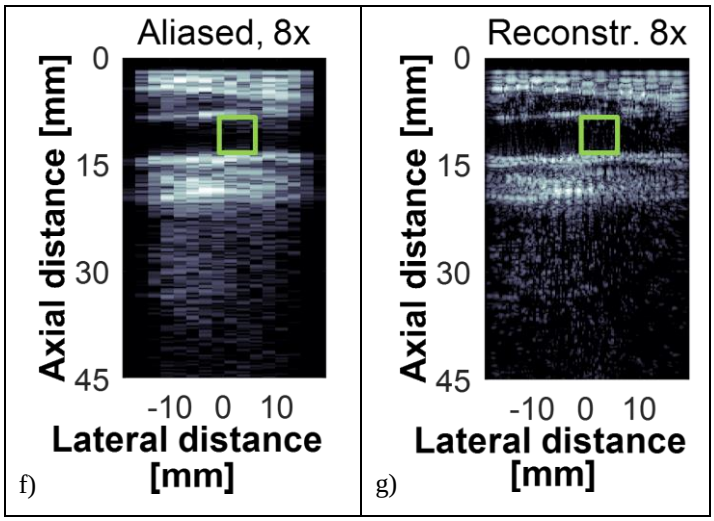

Fig. 2. Imaged original, aliased and reconstructed datasets obtained using second harmonic imaging. The green rectangle denotes the area where the intensty is analyzed in Table II. a) Original dataset. b) Dataset with 2x channel reduction. c) Reconstruction based on dataset with 2x channel reduction. d) Dataset with 4x channel reduction. e) Reconstruction based on dataset with 4x channel reduction. f) Dataset with 8x channel reduction. g) Reconstruction based on dataset with 8x channel reduction.

As can be observed in Fig. 2a, the original image based on second harmonic imaging is sharper – especially around the edges of the blood vessel – compared to the fundamental original image of Fig. 1a. However, the signal-to-noise-ratio of the second harmonic image is lower compared to the fundamental image, which leads to a reduced penetration depth in the former image. The imaged aliased datasets of Figs. 2b, d and f became increasingly washed out and blocky for higher levels of channel reduction. At each level of channel reduction the imaged reconstructed datasets (see Figs. 2c, e and g) were significantly clearer and sharper compared to the imaged aliased datasets. For higher levels of channel reduction the details in the imaged reconstructed datasets became less distinct and the images more grainy. This was caused by the increasing effect of the numerical noise (as a function of the amount of channel reduction) introduced into the images due to the iterative forward and inverse applications of the imaging algorithm. Notice the hyperbola-like artifacts in the near-field of the reconstructed image based on the 8x aliased dataset. Comparing the reconstructions of the 4x aliased datasets imaged using either fundamental or 2nd harmonic imaging shows that the reconstructed 2nd harmonic image is sharper and of significantly higher quality than the fundamental one. A similar conclusion can be drawn for the imaged 4x aliased datasets.

Table II shows the average intensity of the squares in the corresponding figures of Fig. 2.

TABLE II. AVERAGE INTENISTY IN GREEN SQUARES IN FIG. 2

Channel reduction level	**Aliased image [dB]**	**Reconstructed image [dB]**
2x	-47 (Fig. 2b)	-49 (Fig. 2c)
4x	-46 (Fig. 2d)	-48 (Fig. 2e)
8x	-46 (Fig. 2f)	-51 (Fig. 2g)
Original	-50 (Fig. 2a)	

The averaged intensities in the green squares in the imaged reconstructed datasets were lower than the corresponding intensities in the imaged aliased datasets. However, the intensities of the reconstructed datasets for channel reductions of 2x and 4x remained higher than the one of the original dataset, which was caused by the increased blurring of the edges of the bloodvessel in the imaged reconstructed dataset. For the imaged reconstructed dataset with an channel reduction of 8x the intensity in the green square was lower than that of the imaged original dataset. This was however not caused by increased sharpness of the edges, but by a lower overall mean intensity.

Note that the originally recorded datasets were already aliased. The pitch of the array used was 0.3 mm. For fundamental imaging the center frequency was 5 MHz, which yields a wavelength of ~0.3 mm in water. Thus, for fundamental imaging the originally recorded dataset was already 2x aliased in transmission and 2x aliased in reception. For second harmonic imaging the center frequency used for transmission was 3.4 MHz yielding a wavelength of 0.44 mm in water. The corresponding frequency of the 2nd harmonic was 6.8 MHz yielding a wavelength of 0.22 mm. Thus, for second harmonic imaging the originally recorded dataset was already 1.4x aliased in transmission and 2.7x aliased in reception.

V. CONCLUSION

It was feasible to reconstruct channel reduced (aliased) *in-vivo* datasets obtained using second harmonic imaging. The reconstruction algorithm significantly improved the image quality in all cases for both fundamental and second harmonic imaging. It was possible to reconstruct 2x aliased datasets with a minimal loss in image quality compared to the original image for both fundamental and second harmonic imaging. Moreover, it was possible to reconstruct a 4x aliased dataset obtained using second harmonic imaging with only a small loss in image quality.

REFERENCES

[1] P.L.M.J. van Neer, S. Blaak, J.G. Bosch, C.T. Lancée, C. Prins, N. de Jong, *'Mode vibrations of a matrix transducer for three-dimensional second harmonic transesophageal echocardiography'*, Ultrasound Med. Biol., 38(10):1820-1832, 2012.

[2] P.L.M.J. van Neer, A.W.F. Volker, 'Imaging beyond aliasing', *Proc. IEEE Ultrasonics Symp.*, Taiwan, 2015.

[3] P.L.M.J. van Neer, H.J. Vos, A.F.W. Volker, 'Stolt migration based iterative trace reconstruction', *Proc. IEEE Ultrasonics Symp.*, France, 2016.

[4] R. H. Stolt, *Migration by Fourier Transform*, Geophysics, 43(1):23-48, 1978.

[5] G. F. Margrave, *Numerical Methods of Exploration Seismology*, University of Calgary, 2003.